View metadata, citation and similar papers at core.ac.uk

brought to you by CORE

provided by Elsevier - Publisher Connector

Developmental Cell, Vol. 5, 161–174, July, 2003, Copyright ©2003 by Cell Press

Retroviral Genomic RNAs Are Transported to the Plasma Membrane by Endosomal Vesicles

Eugenia Basyuk,[1] Thierry Galli,[2] Marylène Mougel,[3] Jean-Marie Blanchard,[1] Marc Sitbon,[1] and Edouard Bertrand[1,*]
[1]IGMM-CNRS UMR5535
Université Montpellier II
IFR 24
1919, route de Mende
34293 Montpellier Cedex 5
[2]Inserm U536, Paris
[3]CNRS UMR51421, Montpellier
France

Summary

The viral genomes of α- and γ-retroviruses follow an outbound route through the cytoplasm before assembling with the budding particle at the plasma membrane. We show here that murine leukemia virus (MLV) RNAs are transported on lysosomes and transferrin-positive endosomes. Transport on transferrin-positive vesicles requires both Gag and Env polyproteins. In the presence of Env, Gag is rerouted from lysosomes to transferrin-positive endosomes, and virion production becomes highly sensitive to drugs poisoning vesicular and endosomal traffic. Vesicular transport of the RNA does not require prior endocytosis, indicating that it is recruited directly from the cytosol. Viral prebudding complexes containing Env, Gag, and retroviral RNAs are thus formed on endosomes, and subsequently routed to the plasma membrane. This may allow retroviruses to hijack the endosomal machinery as part of their biosynthetic pathway. More generally, tethering to vesicles may provide an efficient mechanism for directed RNA transport.

Introduction

A number of RNAs adopt specific localizations in the cytoplasm of eukaryotic cells, thus allowing the delivery of newly synthesized polypeptides in particular intracellular areas. RNA localization plays critical roles in asymmetrical cell division and in specifying properties of cytoplasmic areas in a wide variety of cells (for reviews, see Kloc et al., 2002; Saxton, 2001). The role of RNA localization is not limited to the modulation of local translation, since noncoding or untranslated RNA species can also be found in specific cytoplasmic compartments. A variety of mechanisms has been shown to govern subcytoplasmic mRNA localization. In most cases, directional RNA transport mechanisms are at play, which use diverse types of molecular motors. For instance, in yeast, Ash1 mRNA particles are transported to the bud site on actin cables by a specific myosin motor (Bertrand et al., 1998). In *Drosophila*, movements of RNA particles toward the apical side of blastocyst cells require microtubules and dynein motors (Wilkie and Davis, 2001). In oligodendrocytes, MBP mRNA movements toward cellular processes require microtubules and kinesin motors (Carson et al., 1997). Interestingly, RNA localization usually involves transport of macromolecular aggregates containing a large number of RNA molecules, often referred to as "particles." The detailed composition of these large structures is not known, and in particular, the cellular compounds that embark with these RNA-containing aggregates have not yet been identified.

During the retrovirus replication cycle, the genomic viral RNA serves both as a protein synthesis template and as a viral genome when packaged. As observed by electron microscopy, α- and γ-retroviruses, as well as lentiviruses such as HIV-1 and -2, assemble at the plasma membrane where virion budding occurs (Freed, 1998; Garoff et al., 1998; and references therein). Completion of virion production therefore requires the genomic viral RNA to migrate to the cell surface. The mechanisms involved in this RNA transport are still unknown (for a discussion, see Ploubidou and Way, 2001), and a specific process is likely at play, since mRNAs have relatively low mobilities in the cytoplasm (Fusco et al., 2003).

Production of infectious retroviral particles requires that viral genomic RNAs are present at the budding sites on the plasma membrane but also requires the concomitant presence of a number of other viral molecules, including Gag and Env polyproteins. Env is a transmembrane protein that reaches the plasma membrane via the secretory pathway. Gag is a cytosolic protein that directly binds cellular membranes through a myristoyl or other amino-terminal anchor (for reviews, see Freed, 1998; Garoff et al., 1998). Gag expressed alone reaches the cell surface independently of membrane trafficking (Suomalainen et al., 1996) and is sufficient to assemble budding virion-like particles at the plasma membrane (Gheysen et al., 1989). However, MLV and HIV envelope proteins confine viral budding to the basolateral side of polarized epithelial cells (Lodge et al., 1997), and at least in rat neurons, they also modulate Gag localization (Weclewicz et al., 1998). Gag might therefore utilize different trafficking pathways when expressed in the context of a whole virus. These data also suggest an interaction between Env and Gag within the cell. The location of this interaction, and whether it is specific to polarized cells, remains unknown. More generally, it is not clear how Gag, Env, and the viral genomic RNA reach common sites at the plasma membrane to assemble, bud, and form virions.

We have addressed these questions with an MLV model system. By imaging single RNA molecules in living cells, we show that Env and Gag tether the RNA onto endosomal vesicles, allowing the resulting complex to be routed to the cell surface.

Results

Visualization of Single Molecules of MLV RNA in Living Cells

To directly visualize retroviral RNA movements in living cells, we used a technique that we recently developed

*Correspondence: bertrand@igm.cnrs-mop.fr

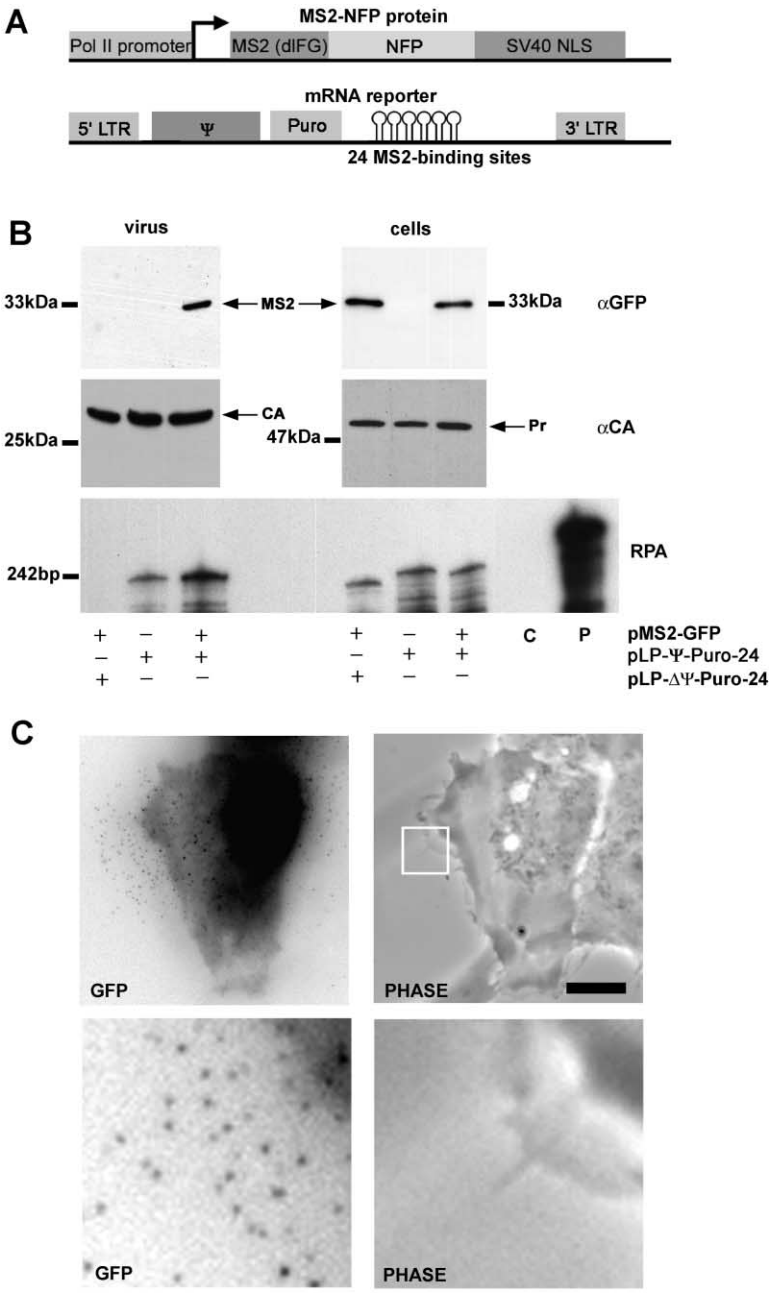

Figure 1. Visualization of Single Molecules of MLV Retroviral RNA in Living Cells

(A) Schematic representation of the constructs.

(B) Binding of the MS2-GFP protein on the reporter RNA does not inhibit its packaging. 293T cells were transfected with various combinations of pCMV-GagPol, pMS2-GFP, and the ms2 reporter containing or not the Ψ packaging sequence (pLP-Ψ-Puro-24 and pLP-ΔΨ-Puro-24, respectively). Cellular and viral fractions were prepared, and proteins and RNA were analyzed by Western blotting and RNase protection, respectively. An antibody against GFP (αGFP) recognized the MS2-GFP fusion (arrow MS2). An αCA antibody (αCA panel) recognized the capsid in virions (arrow CA) and the Gag polyprotein in cells (arrow Pr). The RNA probe (285 nt long, lane P) protected fragments of 240 and 225 nt, on the Ψ-containing and ΔΨ constructs, respectively (RPA panel). Lane C, control yeast RNA.

(C) In situ detection of packaged retroviral RNAs. Fly E packaging cells were cotransfected with pMS2-GFP and pLP-Ψ-Puro-24, and observed live. Left, GFP fluorescence; right, phase contrast. Bottom panels are enlargements of the boxed area. Extracellular fluorescent dots correspond to viral RNAs that have been packaged into virions and released from cells. Bar, 10 μm.

for visualization of single mRNA molecules (Bertrand et al., 1998; Fusco et al., 2003). The technique uses a nuclear MS2-GFP fusion protein and a reporter RNA tagged with 24 MS2 binding sites (ms2). In this case, the viral RNA reporter was based on MLV and contained Mo-MuSV LTRs, the Mo-MLV Ψ packaging signal, and the puromycin gene followed by the ms2 repeats (pLP-Ψ-Puro-24; Figure 1A). To verify that binding of MS2-GFP molecules to the reporter RNA would not affect its packaging into viral particles, we transfected 293T cells with a Mo-MLV Gag-Pol expression vector, the ms2-tagged reporter construct, and an MS2-GFP expression vector (pMS2-GFP). Controls included transfection without the MS2-GFP vector, or with an ms2 reporter that lacked Ψ. Supernatants from transfected cells were collected, viral particles were purified by high-speed centrifugation, and protein and RNA contents were analyzed by Western blotting and RNase protection assays, respectively. All transfected cells produced similar amounts of viral particles, as shown by the amount of Gag-derived capsid protein in the supernatant (Figure 1B, panel αCA). In contrast, the MS2-GFP protein was detected only in virions produced from cells that expressed the ms2 reporter containing Ψ (Figure 1B, panel αGFP). This data demonstrated that the incorporation of the MS2-GFP protein into virions was specifically due to Ψ-dependent packaging of the viral reporter RNA. In addition, similar amounts of ms2-tagged viral RNA was

packaged in cells whether or not the MS2-GFP fusion protein was expressed (Figure 1B, panel RPA), demonstrating that the presence of MS2-GFP did not adversely affect packaging of the viral RNA reporter.

When Fly E packaging cells stably expressing Gag and Env genes were cotransfected with pMS2-GFP and the retroviral RNA reporter and examined in situ, small fluorescent dots were readily detected around the transfected cells (Figure 1C). Extracellular GFP dots were never observed in transfected cell lines which do not harbor Gag, suggesting that these dots corresponded to the ms2-tagged virions released from the cells. Altogether, these results suggested that MS2-GFP could be used to monitor the transport of retroviral RNAs to the plasma membrane and out of the cell.

MLV RNAs Display Directed Movements in Chronically Infected and Packaging Cells

To record movements of MLV genomic RNA in living cells, 3T3 cells chronically infected with replication competent MLV were cotransfected with the ms2-tagged retroviral reporter and pMS2-GFP. The use of chronically infected cells precluded viral reinfection and ensured that only late phases of the viral cycle were observed. Notably, rectilinear movements of the reporter RNA were often observed (Figure 2A). These directed movements transported the RNA over long distances (5.6 $\pm$ 3 μm on average) at velocities of approximatively 1 μm/s (0.8 $\pm$ 0.4 μm/s on average), similar to the speed of fast microtubule-dependent transport. This suggested an active mechanism of RNA transport (Figure 2A). This frequent directional transport over long distances was dependent on the presence of Ψ (Figure 2B), since its frequency decreased about 50 times when Ψ was deleted, from 4.1 $\pm$ 2.4 movements per minute, to 0.08 $\pm$ 0.28. This indicated that directed motions were likely associated with RNA packaging. To test the influence of viral proteins in this process, we analyzed viral RNA transport in human HT1080 cells that expressed no MLV proteins, or in derivatives of these cells that expressed either Gag/Gag-Pol alone (HT-Fly cells) or both Gag/Gag-Pol and Env (Fly E cells). We chose this heterologous human system because it is devoid of endogenous rodent retroviruses that could potentially interfere with MLV RNA transport. In addition, stable cell lines mimic chronically infected cells that constantly express viral proteins, and their use diminishes the risk of artifacts due to protein overexpression as often observed with transient transfections. In HT1080 cells with or without Env, and in HT-Fly cells expressing Gag/Gag-Pol in the absence of Env, the viral reporter RNA behaved similarly to a standard mRNA (Bertrand et al., 1998; Fusco et al., 2003): the RNA was homogeneously distributed in the cytoplasm, and the movements were neither fast nor directional (Figure 2C; data not shown). In contrast, in Fly E cells concomitantly expressing Gag/Gag-pol and Env polyproteins, retroviral RNA molecules concentrated on undefined cytoplasmic structures (Figure 2D), and many also moved rapidly across the whole cell. The mean distance travelled by RNA particles was 4.5 $\pm$ 1.5 μm, and their mean velocity was 1.2 $\pm$ 0.57 μm/s, similar to the values found in chronically infected 3T3 cells. The frequency of movement was higher than in chronically infected cells (13.6 $\pm$ 5.7 movements per minute), possibly due to intrinsic differences between the two cell types or to the lack of competition with wild-type retroviral RNAs for viral proteins. About 20% of the RNA particles displayed abrupt turns or stopped and then moved again. We also noted that movements occurred with a bias toward the cell periphery (68% of the cases). Finally, colcemid or nocodazole, two agents that disassemble microtubules, abolished directed movements, and two-color imaging showed that the RNA was moving on microtubular tracks (Figure 2E; see Supplemental Data at http://www.developmentalcell.com/cgi/content/full/5/1/161/DC1). Thus, when expressed together, Env and Gag directed the retroviral RNA to a cellular transport system. This observation was not particular to Fly E cells, since similar results were obtained with other packaging systems, including murine 3T3-GPE and human TE-A9 cells (data not shown).

MLV RNA Reporters Are Transported on Lysosomes and Transferrin-Positive Vesicles

Env is a transmembrane protein that reaches the plasma membrane via the secretory pathway, while Gag is myristoylated and binds both cellular membranes and the retroviral RNA (for reviews, see Freed at al., 1998; Garoff et al., 1998). Thus, these molecules could link the RNA with vesicular traffic. Upon close examination of RNA localization and transport in chronically infected 3T3 cells and in Fly E cells, the viral RNA indeed appeared to be transported on vesicles (Figures 2A and 2D, inset). In order to define the nature of the vesicles involved in this process, chronically infected 3T3 cells or packaging Fly E cells were transfected with a pMS2-GFP expression vector (pMS2-GFP) and the retroviral RNA reporter, and specific membrane markers were simultaneously labeled in living cells. In both cell lines, the RNA reporter colocalized and was cotransported with markers of the endosomal compartment. This occurred with internalized fluorescent human transferrin, a marker that is endocytosed and transfered to early and recycling endosomes, and with lysotraker, a vital dye that stains late endosomes and lysosomes (Figure 3). Quantitation of the frequency of cotransport in Fly E cells showed that the RNA was predominantly transported on transferrin-positive endosomes (90% of the cases). Live cell imaging also showed that the RNA molecules which colocalized with the vesicles at steady state were attached to them, as indicated by their concomitant movements (Figure 3). Furthermore, at high resolution, it was apparent that the RNA surrounded the vesicles and thus localized on their cytoplasmic face. This demonstrated that these RNAs molecules were not associated with viral particles that were already formed, but rather with nascent virions at an early stage of assembly, well before completion of budding.

Gag and Genomic MLV RNAs Are Associated with Lysosomes and Transferrin-Positive Endosomes in Chronically Infected Cells

To confirm the results obtained with the ms2-tagged reporter RNA, we analyzed the trafficking of the wild-type genomic RNA in chronically infected cells. The

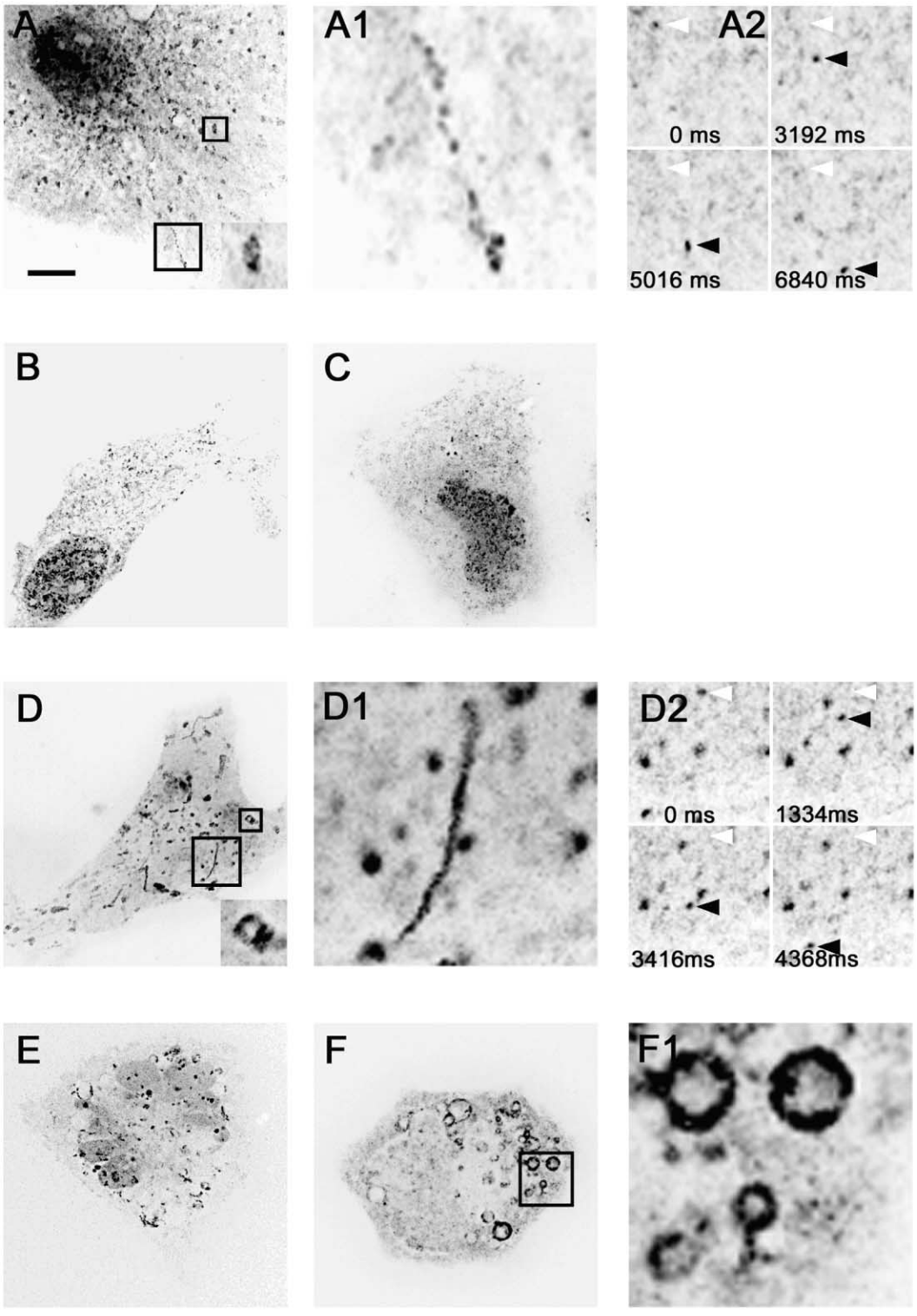

Figure 2. MLV Retroviral RNAs Are Actively Transported in Chronically Infected and Packaging Cells

Cells were transfected with pMS2-GFP and the reporter containing or not the Ψ packaging sequence (pLP-Ψ-Puro-24 or pLP-ΔΨ-Puro-24), and observed live. Images were recorded at a rate of three images per second (for movies, see Supplemental Data at http://www.developmentalcell.com/cgi/content/full/5/1/161/DC1), and maximal image projection of stacks corresponding to about 10 s of the original movies are shown. The tracks of RNA molecules are visible, and directed movements appear as rectilinear lines (see [A] and [D]). The amount of MS2-GFP remaining in the nucleus varies from cell to cell and is not related to the cytoplasmic RNA movements. Bar, 10 μm.

(A and B) The movements of LP-Ψ-Puro-24 (A) and LP-ΔΨ-Puro-24 (B) RNAs in 3T3 cells chronically infected with MLV are displayed. Only the Ψ-containing RNA displays long-distance rectilinear movements. Inset of (A), RNA molecules clustered around a vesicle. (A1) shows an enlargement of the boxed area of (A), while (A2) display the position of RNA molecules at specific times. Position of an RNA molecule is

localization of the RNA was determined by in situ hybridization in fixed cells, together with either a resident lysosomal protein, cystinosin, or fluorescent internalized transferrin. It should be noted that we used a combination of six fluorescent oligonucleotide probes, which together allow for a reliable detection of single RNA molecules. Consistent with the results obtained in living cells, we detected MLV genomic RNAs both on lysosomes and transferrin-positive endosomes (Figures 4A and 4B). Because Gag is responsible for the specific recognition of the viral RNA, our results implied that Gag should also be found on endosomal membranes. Indeed, in fixed, chronically infected 3T3 cells, Gag was frequently found on lysosomes and less frequently on transferrin-positive endosomes (Figures 4C and 4D). Quantitative imaging revealed that 12% of intracellular Gag localized on lysosomes (and nearly all lysosomes contained detectable Gag molecules), while 4% was on transferrin-positive endosomes (only a fraction contained Gag; Figure 6C). The rest of the signal was distributed throughout the cell, including at the plasma membrane. It is important to note here that these values represent the steady-state localization of the protein and that a much larger fraction of the protein likely transit through endosomes during its lifetime. Indeed, blocking endosomal traffic with monensin leads to a strong accumulation of Gag on endosomes (see below).

To confirm the results obtained by microscopy, we undertook a biochemical approach. Vesicular extracts were prepared from chronically infected 3T3 cells, and the material containing Gag or the viral RNA were immunoisolated with anti-Gag antibodies or biotinylated oligonucleotides specific for MLV sequences, respectively. Bound vesicles were then identified by Western blotting with antibodies specific for different endosomal compartments (Figure 5A). In agreement with the microscopy, lysosomes were immunoisolated with both anti-Gag antibodies and anti-MLV oligonucleotides. The amount of vesicles recovered with the oligonucleotides was much less than with the antibodies, probably reflecting the smaller number of molecules of RNA bound to the vesicles. The isolation was however specific since an oligonucleotide complementary to a snoRNA and that had a similar T_m did not allow recovery of any of the markers analyzed. In addition to lysosomes, vesicles containing the transferrin receptor, a plasma membrane protein that constantly cycles through early and recycling endosomes, were also efficiently isolated. It should be noted that broken pieces of the plasma membrane should not be isolated by this procedure since they predominantly generate vesicles with Gag located at their inside and inacessible to antibodies (Suomalainen et al., 1996). Furthermore, we also isolated large amounts of vesicles containing cellubrevin, a SNARE protein involved in membrane fusion events and localized on recycling endosomes (Galli et al., 1994). Altogether, these data unambiguously demonstrated the tight physical association of Gag and the viral RNA with the endosomal compartment in chronically infected cells. This also demonstrated that these viral complexes were at an early stage of assembly since they were accessible to antibodies and hybridization.

Env Sensitizes Exit of Viral Particles to Drugs Poisoning Vesicular Traffic

To gain direct evidence that vesicular traffic was important for viral RNA transport and packaging, we tested the effects of well-characterized inhibitors of membrane trafficking. 3T3 cells chronically infected with MLV were treated with the following drugs: colcemid or nocodazole, which depolymerize microtubules and block motorized vesicular transport; monensin, a monovalent ion-selective ionophore that neutralizes acidic intracellular compartments such as the trans-Golgi apparatus cisternae, lysosomes, and endosomes, leading to defects in vesicular budding; and brefeldin A (BFA), which inhibits Arf GTPase cofactors and leads to Golgi disassembly as well as perturbation of the endosomal system. Virions were purified, and the amount of retroviral RNA present in the viral fraction was determined by RNase protection assays. Colcemid, nocodazole, monensin, and BFA all decreased by 70%–80% the amount of retroviral RNAs released from cells (Figure 5B, panel RPA). In contrast, the amount of retroviral RNA within the cells remained the same or even increased, suggesting that a significant fraction of the viral RNA utilized a vesicular pathway to exit chronically infected cells.

We then analyzed the trafficking of Gag. In chronically infected 3T3 cells, as well as in Fly E packaging cells, colcemid and monensin reduced the amount of Gag released in the viral fraction (Figures 5B and 5C, panels αCA). This result indicated that, similar to the RNA, Gag required vesicular transport to exit the cells. Surprisingly however, in HT-Fly cells that express Gag but not Env, colcemid and monensin had only a very modest effect on Gag release (Figure 5C). These results were consistent with previous reports showing that when expressed alone, Gag can reach the plasma membrane by diffusing through the cytosol (Suomalainen et al., 1996). In addition, this was also coherent with the inhibitory effect of monensin that was previously observed in Psi2 packaging cells expressing a Gag-β-galactosidase fusion protein (Hansen et al., 1990). The fact that Env sensitized viral release to drugs blocking vesicular traffic suggested that the retroviral RNA and Gag were transported in a complex with Env to the cell surface. In agreement

indicated at t = 0 (white arrowhead) and at the indicated time points (black arrowhead).

(C and D) The movements of LP-Ψ-Puro-24 RNA in HT-Fly cells (C) and Fly E cells (D) are displayed. Only Fly E cells expressing both Gag and Env show a high frequency of long-distance directed movements. In (D), the inset shows an enlargement of the upper box, with RNA molecules clustered around a vesicle. (D1) shows an enlargement of the bottom box of (D), while (D2) displays the position of RNA molecules at specific times.

(E) Fly E cells have been treated with 10 μM colcemid for 1 hr, and no rectilinear long-distance movement is observed. Note that the nucleus of Fly E cells is often not round but takes a multilobular shape (see also the other figures).

(F) Fly E cells have been treated with monensin (10 μM for 3 hr), and RNAs accumulate on enlarged vesicles. (F1) shows an enlargment of the boxed area in (F).

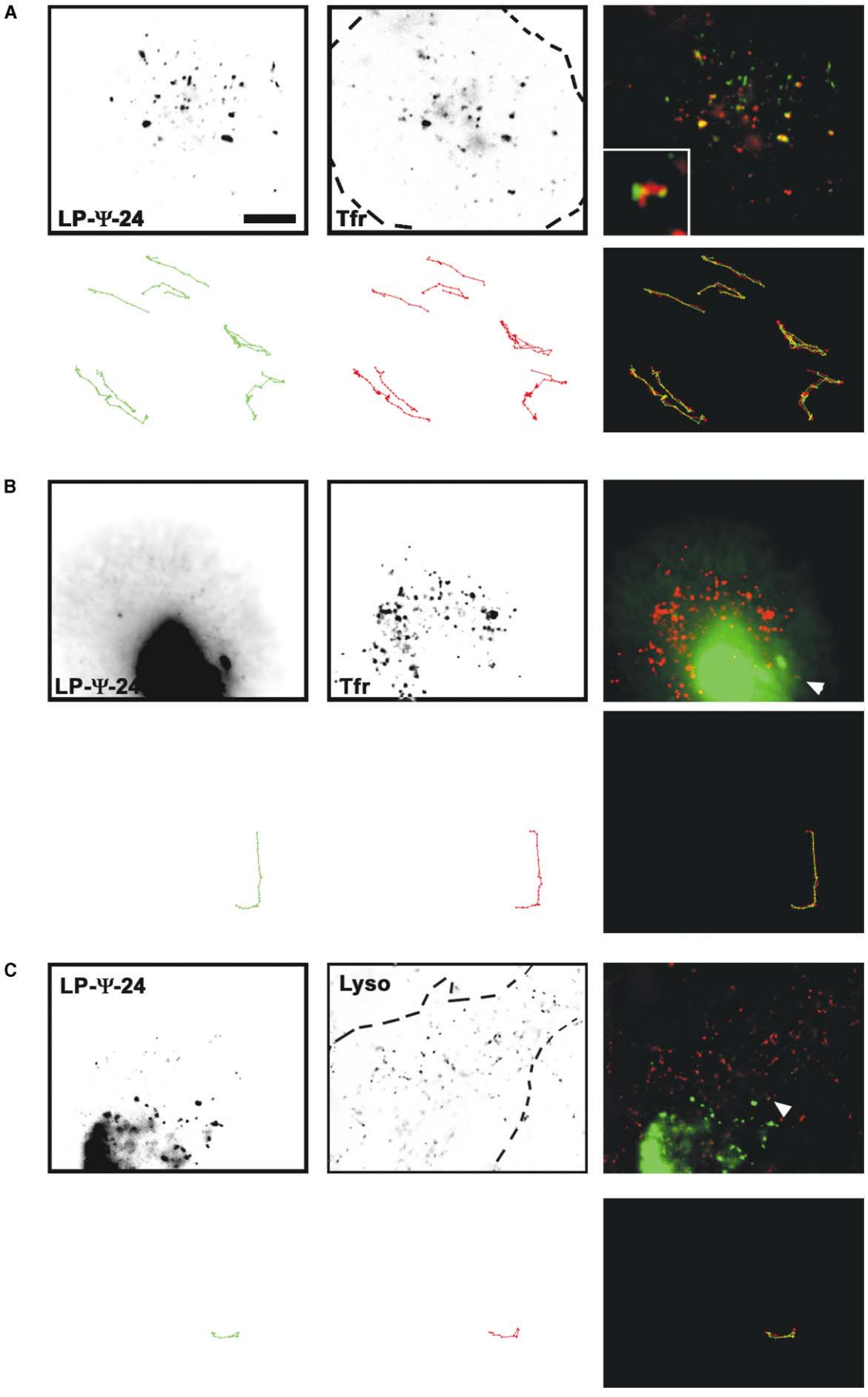
A
LP-Ψ-24
Tfr
B
LP-Ψ-24
Tfr
C
LP-Ψ-24
Lyso

with this idea, we found that in chronically infected cells, Env localized to early and recycling endosomes, as well as on lysosomes, similar to the localization of the viral RNA and Gag (see Supplemental Data at http://www.developmentalcell.com/cgi/content/full/5/1/161/DC1). Taken together, our data suggested that viral complexes used vesicular traffic to exit cells.

To further document the action of the drugs, we analyzed their effect on the localization and movements of the retroviral RNA reporter. Colcemid and nocodazole both blocked motorized RNA movements (Figure 2E; data not shown); while upon monensin treament, the RNA accumulated around intracellular vesicles (Figure 2F). Similarly, in chronically infected 3T3 cells, monensin induced a drastic relocalization of the viral components since both Gag and Env became strongly enriched on lysosomes (Figure 6C; see Supplemental Data at http://www.developmentalcell.com/cgi/content/full/5/1/161/DC1 Data). Indeed, as much as 65% of the total amount of cellular Gag colocalized with lysosomes in this case (compared to 12% in untreated cells). In addition, the colocalization with lysosomes was specific since a Rab11-GFP did not colocalize with either Gag or Env in the same conditions. Thus, the drugs not only inhibited the exit of the virus but also had a direct effect on viral RNA transport and on the trafficking of the other viral components.

Env Relocalizes Gag from Lysosomes to Transferrin-Positive Endosomes

To gain further insights into the trafficking of Gag, we studied its localization by immunofluorescence in HT-Fly and Fly E cells. In HT-Fly cells, Gag was highly enriched on lysosomes and only rarely detected on transferrin-positive endosomes (Figure 6A). In contrast, in Fly E cells, Gag was readily detected on transferrin-positive endosomes and less frequently on lysosomes (Figure 6B). To exclude a clonal variation between the two cell lines, we transiently expressed Env in HT-Fly cells, together with a cystinosin-GFP plasmid, to identify transfected cells. We found that indeed Env expression was sufficient to relocalize Gag out of lysosomes (Figure 6A). Quantitative imaging showed that in HT-Fly cells, 62% of the intracellular Gag localized on lysosomes and only 2% on transferrin-positive endosomes (Figure 6C). In contrast, in Fly E cells or in HT-Fly cells expressing Env, only 6.5% and 11% of Gag was found on lysosomes, respectively, while as much as 9% localized on transferrin-positive endosomes in Fly E cells. Thus, Env induced a redistribution of Gag from lysosomes to transferrin-positive endosomes.

MLV Reporter RNAs Are Frequently Transported on Rab11-Positive Vesicles

At least two routes exist to go from transferrin-positive endosomes to the plasma membrane. Membrane-bound proteins can exit early sorting endosomes via a Rab4 route or can leave recycling endosomes via a Rab11 pathway (Somsel Rodman and Wandinger-Ness, 2000). To define more precisely the route taken by the retroviral RNA, we labeled it with MS2-YFP while the Rab proteins were tagged with CFP. In live Fly E cells, the RNA colocalized and was often transported with Rab11-positive vesicles (Figure 7A). In contrast, the RNA rarely colocalized with Rab4-positive vesicles and was excluded from these vesicles during its transport (see Supplemental Data at http://www.developmentalcell.com/cgi/content/full/5/1/161/DC1). Quantification of the number of cotransport events showed that 75% occurred on Rab11-positive vesicles ($n = 16$). Thus, the RNA likely reached the plasma membrane via the Rab11 route.

To gain functional insights into the trafficking of the viral RNA through the recycling endosomal compartment, we specifically perturbed membrane fusion events of this compartment with tetanus neurotoxin (TeNT). Indeed, the light chain of TeNT is a highly specific protease that cleaves cellubrevin, a SNARE protein localized on the recycling endosomal compartment in nonneuronal cells (Galli et al., 1994). TeNT also cleaves VAMP-1 and -2, but expression of these proteins is limited to a few cell types (neural cells, muscle cells, and adipocytes). Transfection of Fly E cells with a plasmid expressing TeNT light chain showed that it inhibited about 2-fold the exit of an MLV reporter RNA (Figure 5D). Thus, the RNA molecules traveling on recycling endosomes were on their way out of the cell.

Vesicular Transport of MLV RNAs Precedes Binding to the Plasma Membrane

Association of retroviral RNAs with vesicles could result from either direct recruitment from the cytosol, routing from the Golgi network, or endocytosis of RNAs already localized at the plasma membrane. To discriminate between these possibilities, we first tested whether we could detect retroviral RNAs associated with the Golgi apparatus. No significant association could be detected between a Rab6-CFP marker and the viral RNA in Fly E cells, and the reporter was in fact most often excluded from the Golgi area (see Supplemental Data at http://www.developmentalcell.com/cgi/content/full/5/1/161/DC1). We then analyzed the effect of inactivation of the endocytic machinery. To this aim, Fly E cells were

Figure 3. MLV RNA Reporters Are Transported on Endosomal Vesicles

Cells transfected with pMS2-GFP and pLP-Ψ-Puro-24 were labeled with fluorescent Cy3-transferrin (A and B), or with Lysotracker (C), and imaged live in two wavelengths (for movies, see Supplemental Data at http://www.developmentalcell.com/cgi/content/full/5/1/161/DC1). Green, RNA reporter (LP-Ψ-24); red, fluorescent transferrin (Tfr) or Lysotracker (Lyso).

(A) Fly E cells. Top panels correspond to a single movie frame. Bottom panels show the trajectories of seven RNA particles transported by transferrin-positive vesicles during a 5 min movie. The dots represent the position of the objects at each time point. Bar, 10 μm. The apparent frequency of RNA-directed movements is lower than in Figure 2 due to the slower frame rate used for bicolor imaging. Indeed, only the slowest and longest movements can be identified in these conditions.

(B and C) RNA transport on transferrin-positive endosomes (B) and lysosomes (C) in chronically infected 3T3 cells. The arrowhead points to actively transported RNA particles.

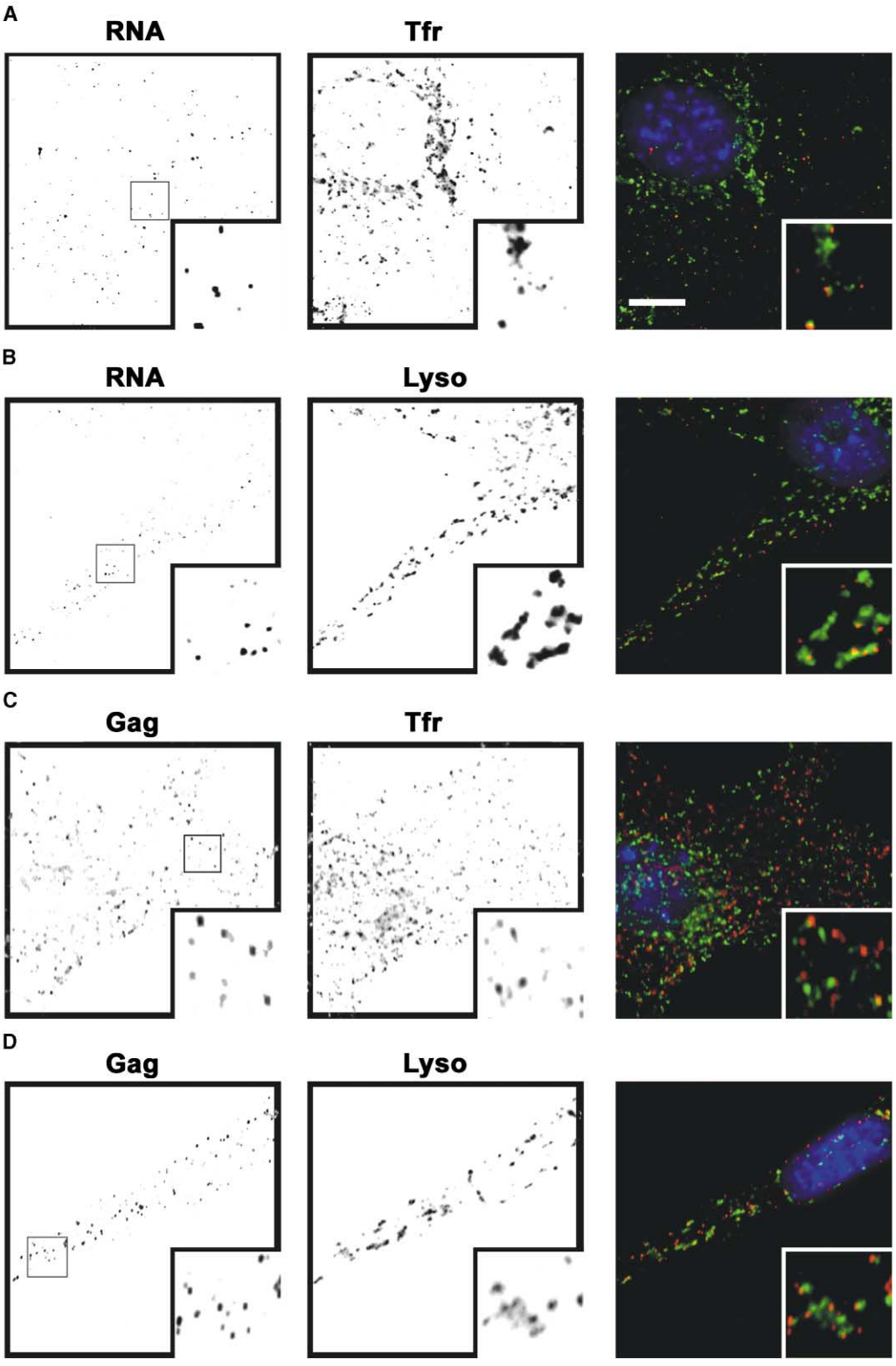

Figure 4. Gag and the Genomic Retroviral RNA Are Associated with Lysosomes and Transferrin-Positive Endosomes in Chronically Infected 3T3 Cells

Gag was labeled by immunofluorescence with αCA antibody (Gag panels, red), and the genomic RNA by in situ hybridization (RNA panels, red). Lysosomes were labeled by stable transfection of a cystinosin-GFP fusion (Lyso panels, green), while transferrin-positive endosomes were labeled with fluorescent transferrin (Tfr panels, green). Insets show magnifications of the boxed areas. Bar, 10 μm.

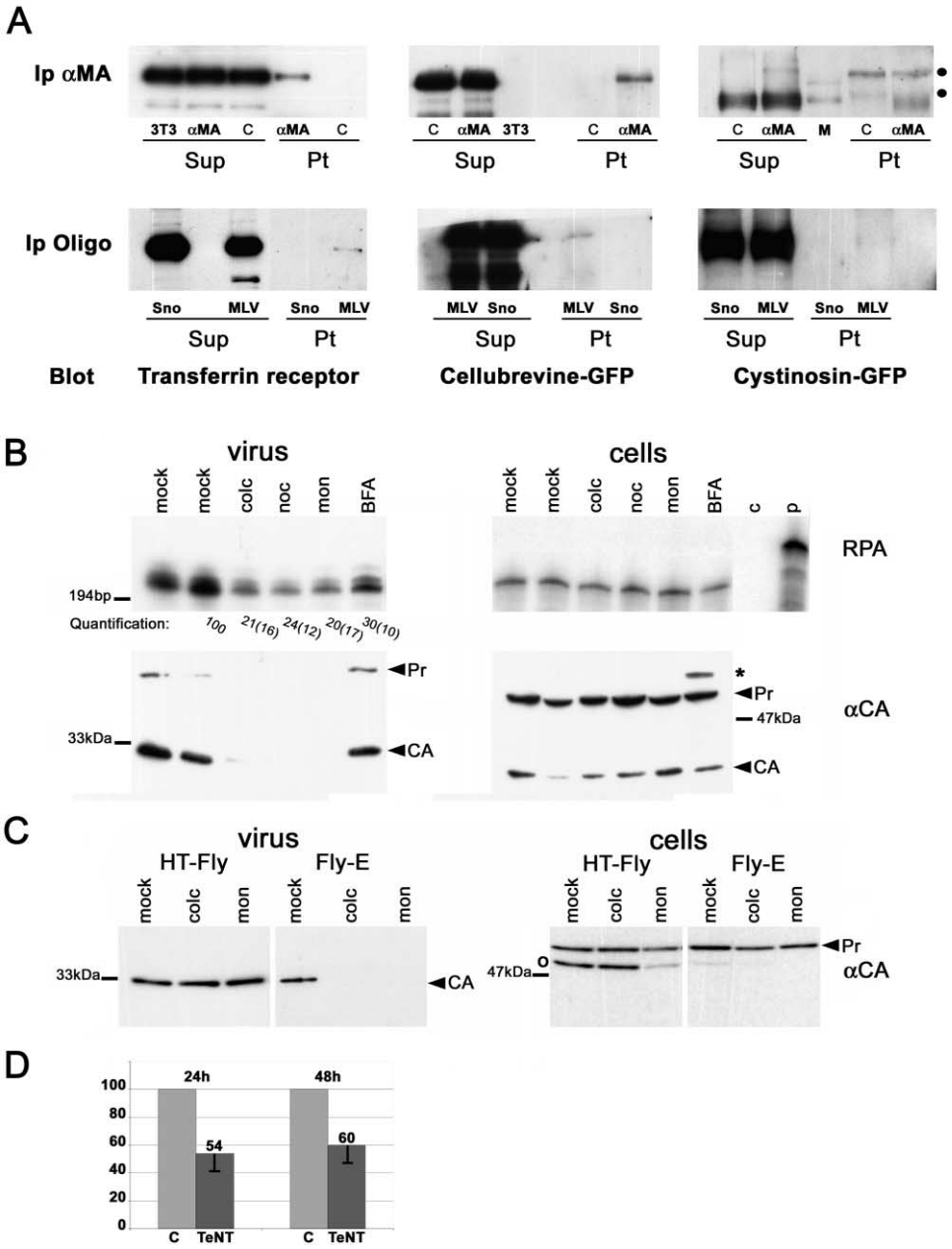

Figure 5. Gag and the Viral RNA Exit Cells via an Endosomal Pathway

(A) Immunoisolation of endosomal vesicles with anti-Gag antibodies (Ip αMA panels) or oligonucleotides complementary to MLV genome (Ip Oligo panels). Chronically infected cells were transiently transfected with a cellubrevine-GFP vector, or were stably transfected with a cystinosin-GFP plasmid, and Western blots of affinity-isolated vesicles were probed with anti-transferrin or anti-GFP antibodies. Sup, supernatant; Pt, pellet. The amount of supernatant loaded corresponded to 20% of the pellet for the transferrin receptor and cellubrevine-GFP, and to 80% for cystinosin GFP. Protein G beads were coated with αMA antibody (αMA lanes) or used directly (C lanes). Streptavidin beads were coated with oligonucleotides complementary to MLV (MLV lanes), or to a snoRNA (Sno lanes). 3T3, extract of nontransfected cells; M, marker. The two dots indicate nonspecific bands that were also obtained with protein G beads alone.

(B and C) Pharmacological inhibition of vesicular traffic inhibits virion release. 3T3 cells chronically infected with MLV (B) and Fly E or HT-Fly cells (C) were treated with the indicated drugs (colc, colcemid; noc, nocodazole; mon, monensin; BFA, brefeldin A; mock, duplicates of untreated cells). The viral and cellular fractions were purified and analyzed by RNase protection (RPA panel) or Western blotting (αCA panels). P, probe; C, control yeast RNA. Viral capsid protein, arrow CA; polyprotein Gag, arrow Pr. In 3T3 cells treated with BFA, glycoGag accumulated (star) due to disruption of Golgi functions. This viral protein is not expressed in HT-Fly and Fly E cells, but a Gag degradation product was present (open circle).

(D) Inhibition of RNA packaging by the catalytic subunit of tetanus toxin. Fly E cells were transfected with a packaged MLV reporter (pLNCX) and a plasmid expressing the catalytic subunit of tetanus toxin. RNAs in the viral fraction were quantified 24 and 48 hr following transfection, normalized to that of the cellular fraction, and plotted as percent of control transfections with a plasmid devoid of the toxin (TeNT, toxin; C, control). Numbers are averaged from two experiments done in triplicate. Bars are the standard deviation.

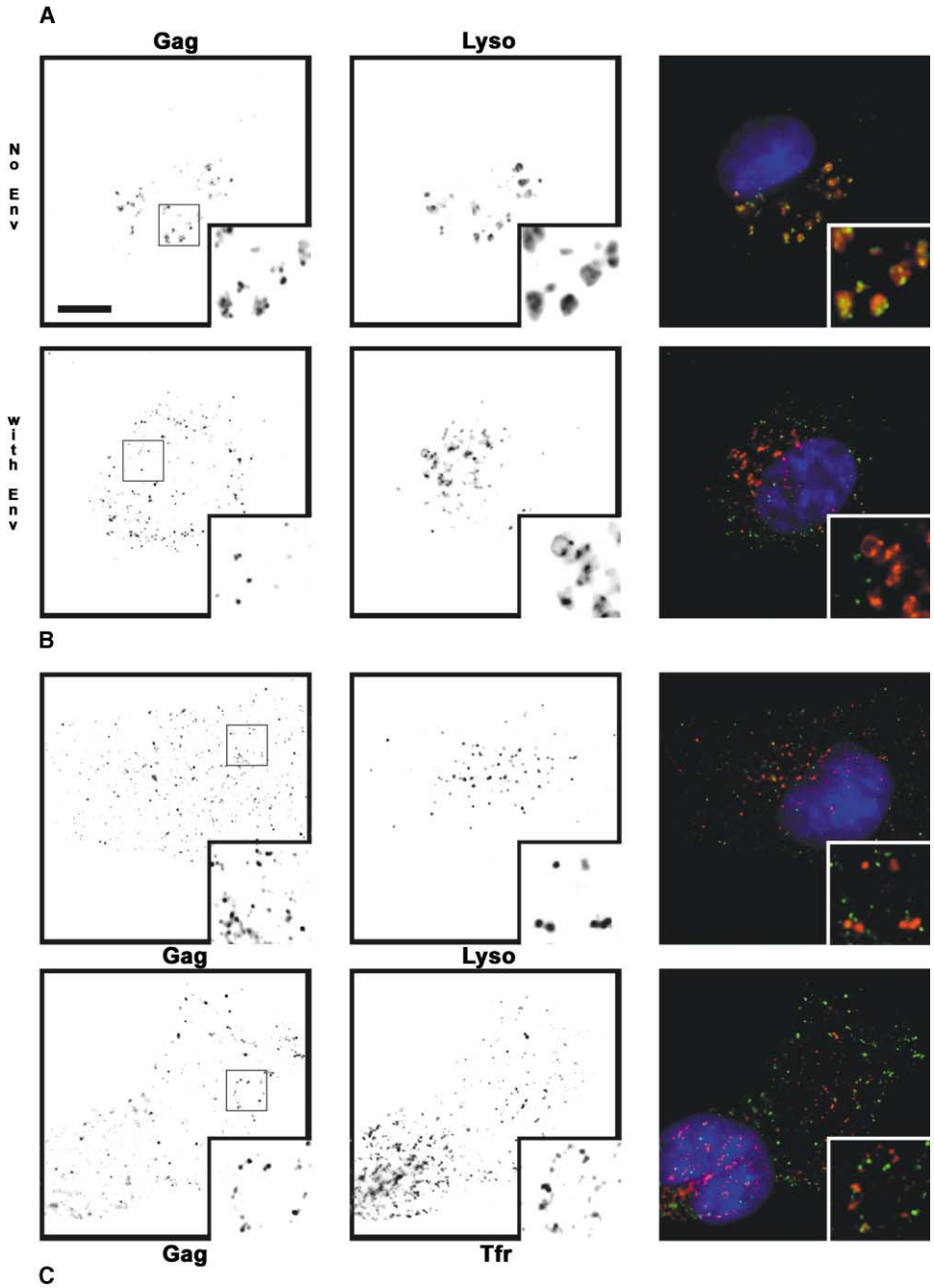

	3T3	3T3/Mon	HT-Fly	HT+Env	Fly-E	cont
Tfr	4% (1.6)	-	2% (2.5)	-	9% (2.7)	0.2% (0.2)
Lyso	12% (8.5)	64% (7)	62% (19)	11% (9)	6.5% (8)	0.4 (0.3)

Figure 6. Env Relocalizes Gag out of Lysosomes and on Transferrin-Positive Endosomes

(A) HT-Fly cells were labeled by immunofluorescence with αCA antibody (Gag panels, green). Upper panels, lysosomes were labeled with Lysotracker (Lyso panels, red). Lower panel, HT-Fly cells were cotransfected with a cystinosin-GFP vector (Lyso panels, red) and a vector expressing Env.

(B) Fly E cells were labeled with αCA antibody (Gag panels, green). Transferrin was labeled with Cy3 (Tfr panels, red), and lysosomes with Lysotracker (Lyso panels, red). Insets show magnifications of the boxed areas. Bar, 10 μm.

(C) Quantification of the amount of intracellular Gag on various endosomal compartments (percent of total intracellular Gag). Cont, control (see Experimental Procedures). Standard deviation in parenthesis.

transfected with a dominant-negative version of Eps15 that inhibits clathrin-mediated endocytosis (Benmerah et al., 1999). To identify cells in which endocytosis was effectively blocked, cells were incubated with fluorescent transferrin before imaging. Importantly, the retroviral RNA reporter displayed rapid, directed movements over long distances in cells that had a strong inhibition of transferrin internalization, indicating that it was still tethered to vesicles (Figure 7B). Thus, RNAs were directly recruited from the cytosol to endosomal membranes without prior binding of the plasma membrane.

Discussion

A Vesicular Model for the Transport of Genomic Retroviral RNAs to the Plasma Membrane

Our data reveal a model for the intracellular transport of MLV RNA (Figure 7C). In this model, a complex between Env and Gag formed at the level of endosomal or lysosomal membranes recruits MLV genomic RNA directly from the cytosol. This occurs by direct binding of vesicular Gag to the Ψ-containing RNA, or by recruitment of a preformed cytosolic Gag-RNA complex through Gag-Gag interactions. The resulting complex is then routed by vesicular traffic to the plasma membrane, where nascent virions complete assembly and bud. Intracellular routing appears to involve Rab11 and the recycling endosomal compartments, and transit through this compartment is dependent on Env. In support of this model, we have observed that: (i) vesicular RNA transport precedes binding to the plasma membrane, indicating that RNAs are recruited on endosomes directly from the cytosol; (ii) the RNAs are present on the cytoplasmic side of vesicles, and thus correspond to virions at an early stage of assembly; (iii) retroviral RNAs are transported in a Gag- and Env-dependent manner on Rab11-positive endosomal vesicles; (iv) Env relocalizes Gag from lysosomes to transferrin-positive endosomes, and in this context, virion production is highly dependent on vesicular transport; and (v) perturbation of membrane fusion events at the interface between recycling endosomes and the plasma membrane inhibits exit of the viral RNA.

Several possible scenarios could account for the localization of Gag and Env on lysosomes and transferrin-positive endosomes (Figure 7C). Env could be routed to endosomes directly from the Golgi apparatus or endocytosed from the plasma membrane. Specific targeting signals may also allow Env to travel back and forth between the Golgi, the plasma membrane, early and recycling endosomes, and lysosomes (Lippincott-Schwartz and Fambrough, 1987; Somsel Rodman and Wandinger-Ness, 2000). Gag likely reaches lysosomes independently of Env, either by direct binding from the cytosol or following endocytosis at the plasma membrane. Indeed, Gag accumulates to high levels in lysosomes when expressed alone (62% of the total cellular Gag, compared to 6% in cells expressing Env). This lysosomal fraction of Gag may be degraded. Alternatively, it may return to the cell surface by direct fusion of lysosomes with the plasma membrane (Reddy et al., 2001). Importantly, our results show that Env has an important role in routing Gag out of lysosomes and toward the recycling endosomal compartment. This route could involve either the Golgi or the plasma membrane (Figure 7).

Indirect evidence has suggested that MLV Gag can traffic on vesicles and that Gag and Env can interact within the cell (Hansen et al., 1990; Lodge et al., 1997; Weclewicz et al., 1998). Our data show that Env and Gag can indeed interact on lysosomes and transferrin-positive endosomes. Because both Gag and the envelope proteins of SIV and HIV-1 and -2 possess endosomal targeting signals (Egan et al., 1996; Garrus et al., 2001), it is very likely that in these cases as well, assembly of early viral complexes occurs on endosomes, with subsequent routing toward the cell surface. Assembly of Gag and Env on endosomes could allow Env to sort Gag within the cell and to control polarized budding (Lodge et al., 1997; Weclewicz et al., 1998), which is known to be very important for viral spreading in animals (Perotti et al., 1996). It is also interesting to note that MLV Env does not appear to increase the number of viral particles produced. This suggests that its role is rather qualitative: to produce virions in the right place and thus increase the chances to encounter target cells.

Virion Biogenesis on Endosomal Membranes

It is likely that the transport of genomic RNAs and Gag by endosomal vesicles functions not only to bring the viral RNA to the plasma membrane but also reflects a more intimate relationship with endosomes. Indeed, the PTAP and PPPY motifs of several Gag proteins are required for late events in virion release and have been shown to function by interacting with proteins involved in endosomal targeting, such as Tsg101 and Nedd4 (Garrus et al., 2001; Strack et al., 2000). It is thought that these interactions allow Gag to divert the budding machinery of multivesicular bodies to the plasma membrane (Garrus et al., 2001). The finding that both Gag and the retroviral RNA depend on endosomes for their transport to the plasma membrane suggests that retroviruses hijack endosomes as part of their biosynthetic pathway. In particular, Gag could recruit the budding machinery of multivesicular bodies by passing through the relevant endosomal membranes, in agreement with our finding that a sizeable fraction of Gag is found on the surface of late endosomes and lysosomes in chronically infected cells. Similarly, budding HIV-1 particles have been found in MHC II-maturing compartment in macrophages, a specialized compartment related to multivesicular bodies (Raposo et al., 2002). The fact that both Env and Gag become blocked on lysosomes following monensin treatment suggest that transit through this compartment is indeed important.

Vesicles as RNA Carriers

Intracellular membranes have developed highly sophisticated mechanisms both to define intracytoplasmic compartments and to efficiently transport molecules to these compartments. Membrane trafficking could therefore be a powerful mean to mediate cytoplasmic RNA localization. An interesting illustration of this potential is the Vg1 mRNA in *Xenopus* oocytes, which is transported to the vegetal pole with a specialized region of the endoplasmic reticulum (for review, see Kloc et al., 2002). Another example is the recent finding that Rab11 is required for the posterior localization of Oskar mRNA in *Drosophila* oocytes. In this case, Rab11 maintains a

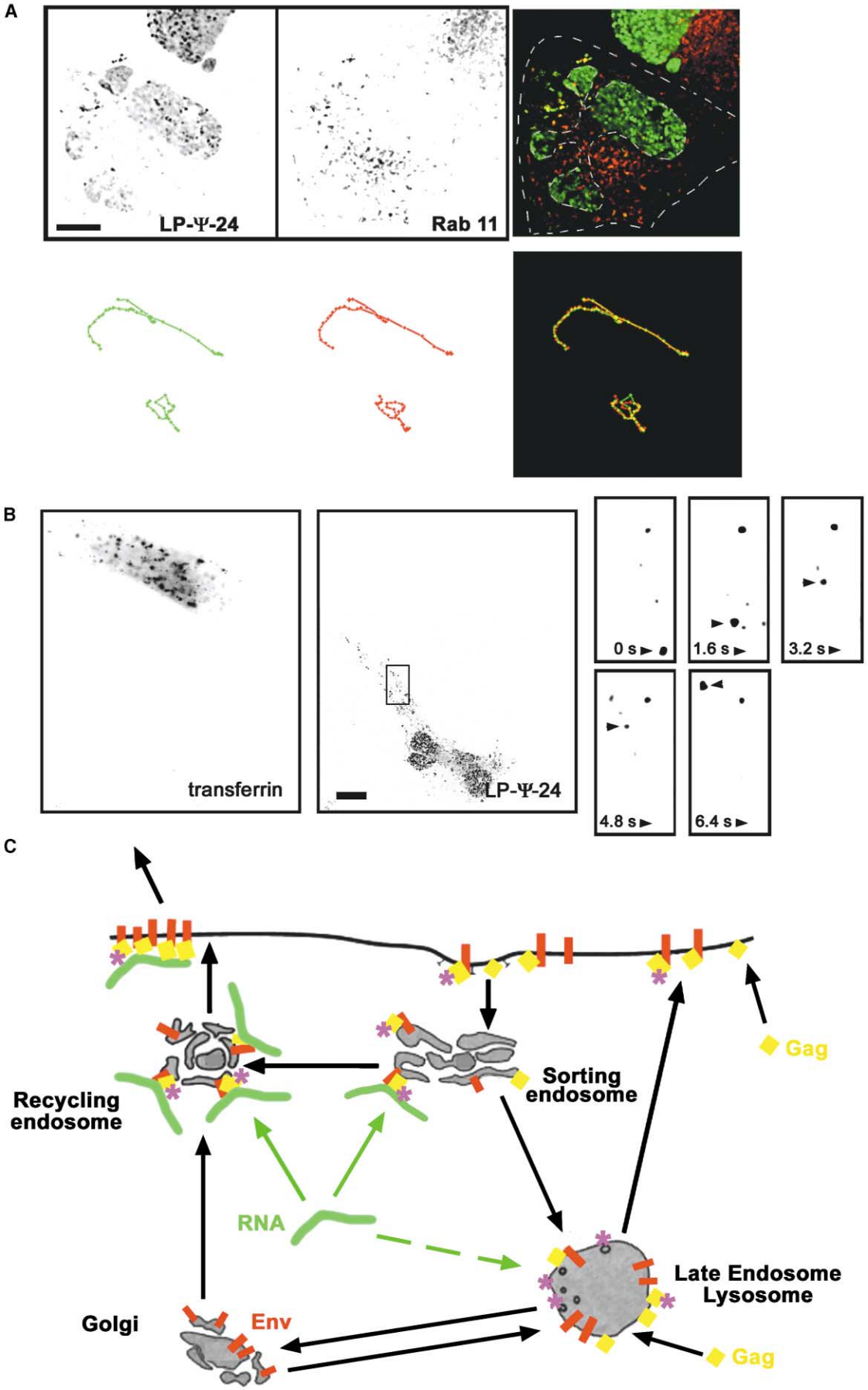
A
LP-Ψ-24
Rab 11
B
transferrin
LP-Ψ-24
0 s
1.6 s
3.2 s
4.8 s
6.4 s
C
Gag
Sorting endosome
Recycling endosome
RNA
Late Endosome Lysosome
Golgi
Env
Gag

specialized membranous domain at the posterior pole, even in the absence of microtubules (Jankovics et al., 2001). The data presented here reinforce the link between RNA localization and membrane trafficking, and reveal an unexpected way to achieve RNA transport, in which adaptor proteins link the RNA to a vesicular transport system.

Utilization of cellular transport machineries by pathogens, including viruses, is a recurrent theme. Indeed, a number of viruses were shown recently to use microtubule-based systems to move within the cell (reviewed in Smith and Enquist, 2002). In the case of retroviruses, it is important to note that this can occur both during cellular exit, as proposed here, and during infection, as shown recently by the finding that HIV-1 genome is transported on microtubular tracks by dynein (McDonald et al., 2002). The dependency of retroviral particles release on the exocytic machinery could open new avenues for the control of viral infections.

Experimental Procedures

Plasmids

pLP-Ψ-Puro-24 was generated by blunt-end cloning of the ms2x24 repeat (from pSL-ms2x24) (Bertrand et al., 1998; Fusco et al., 2003), between the NcoI and Bam HI sites of pLNCX (Clontech, Palo Alto, CA). Plasmid pLP-ΔΨ-Puro-24 was obtained by deleting the sequences of pLP-Ψ-Puro-24 comprised between the Msc I sites. Nuclear pMS2-NFP plasmids were described previously (Bertrand et al., 1998; Fusco et al., 2003), as well as the Moloney MLV Gag and Env expression vectors. Eps15 mutant EΔ95/295 was a gift of A. Benmerah (Benmerah et al., 1999), but the GFP moeity was removed. Plasmid pLNCX is from Invitrogen. The synthetic gene encoding the tetanus toxin light chain TeNT-LC was already described (Eisel et al., 1993).

Cells and Viruses

Human HT1080 cells and their derivatives expressing Moloney MLV Gag (HT-Fly), or both Gag and the ecotropic Moloney MLV Env gene (Fly E), were a gift of F.-L. Cosset and grown as described previously (Cosset et al., 1995). Chronically infected 3T3 cells were obtained by cultivating 3T3 cells infected with Friend MLV viruses for more than 15 days. Cells were transfected by the calcium-phosphate method or with LT1 (Mirus, Madison, WI), and split once before analysis. To label early and recycling endosomes, cells were incubated in DMEM containing 1% serum for 4 hr at 37°C, and then in the same media containing 20 μg/ml of Cy3-labeled transferrin for 45 min at 37°C. To label lysosomes, cells were incubated for 1 hr at 37°C with 0.2 μM Lysotracker-Red (Molecular Probes, Leiden, The Netherlands).

Viruses were prepared by 0.45 μm filtration of cell culture supernatant, followed by high-speed centrifugation (20,000 × g, 2 hr). RNAs were purified with Trizol (Invitrogen) or proteinase K/SDS treatment followed by phenol extraction and ethanol precipitation. They were analyzed by slot-blot hybridization or RNase protection assays. The probes were specific for either pLNCX or Friend MLV. For protein analysis, cells or viruses were resuspended in Laemmli buffer and subjected to Western blotting.

The drugs were used at the following concentration: colcemide, 10 μM; nocodazole, 10 μM; monensin, 5 μM; and BFA, 10 μg/ml. Results shown in Figure 5 were obtained following overnight treatment of the cells, but similar results were obtained after 3 hr of incubation with 30 min of pretreatment (data not shown). Kinetic analysis in Fly E cells also showed that virion exit was blocked 1 hr after addition of monensin (data not shown).

Live Cell Imaging

Using a nonfluorescent cell-culture media (Fusco et al., 2003), cells were plated on a gelatin-coated glass coverslip and mounted in an FCS2 chamber (Bioptechs, Butler, PA). Observations were performed with a Leica DMRA upright microscope equiped for epifluorescence. Images were captured with CCD cameras: either ORCA-100 (Hamamatsu Photonics) or Cool-snap HQ (Roper Scientific). When required, a high-speed wavelength changer was used (DG4; Roper Scientific). Two-dimensional time series and three-dimensional images were deconvolved using Huygens2 (Bitplane).

Motion analysis was done as previously described (Fusco et al., 2003), except that we concentrated on directed movements. Movement frequency was calculated by counting the number of directed motion per minute. Only movements longer than 3 μm were taken into consideration, and the total movie time was 10–20 min (about 15 cells), with a frame rate higher than three images per second. The standard deviation is given from a cell to cell basis. For bicolor movies, we counted the number of cotransport events versus the total number of directed motions.

Antibodies and In Situ Detection of Molecules

Cells were washed once in PBS, fixed for 20 min in PBS containing 4% paraformaldehyde, and permeabilized for 5 min at 4°C in PBS containing 0.05% Triton. Antibody αCA was diluted 1:100 in PBS containing 1% BSA before use. Incubation was performed for 1 hr at 37°C, and unbound molecules were removed by two washes in PBS for 15 min. α-GFP was purchased from Roche Diagnostics; αCA (monoclonal R187 against the capsid part of Gag), monoclonal α-Env (H48), and polyclonal α-Env (805-24) were kind gifts of B. Chesebro.

Detection of RNA in fixed cells was performed by in situ hybridization as previously described (Fusco et al., 2003), with a mixture of six Cy3-conjugated oligonucleotides.

Quantitative Fluorescent Imaging

A series of 3D, deconvolved images of Gag in fixed cells were taken together with a marker for either transferrin-positive endosomes or lysosomes. The images of the marker were then used to create 3D masks, and the masks were used to create a novel 3D image containing only the fraction of Gag associated with the marker. The percent of Gag on the given compartment was then calculated by dividing the total fluorescent of Gag in the masked image by the one contained in the original image. To ensure reliability, we used an automated procedure with identical values of background and threshold between comparable sets of images. In each case, about ten cells were counted. As controls, we did a similar analysis with images of Gag and markers originating from different cells, and which give the degree of colocalization obtained by chance.

Figure 7. Endosomal MLV RNAs Are Recruited from the Cytosol and Transported on Rab11 Vesicles

(A) Retroviral RNA movements on Rab11 vesicles. Fly E cells were cotransfected with pMS2-YFP, pLP-Ψ-Puro-24, and pRab11-CFP. Cells were imaged live in two wavelengths (for movies, see Supplemental Data at http://www.developmentalcell.com/cgi/content/full/5/1/161/DC1). Green, RNA reporter; red, Rab11. The dashed line draws the shape of the cell and of the nucleus. Top panels correspond to a single movie frame. Bottom panels show the trajectories of three RNA particles transported with Rab11 vesicles.

(B) Inhibition of endocytosis does not block RNA transport. Fly E cells were cotransfected with pMS2-YFP, pLP-Ψ-Puro-24, and a dominant-negative mutant of Eps15. Cells were also labeled with fluorescent Cy3-transferrin. Left two panels correspond to transferrin and to the maximal projection of an 8 s movie of the RNA, respectively. Right panels show a time series of an actively transported viral RNA and correspond to the boxed area on the panel "LP-Ψ-24." Arrows point to the initial position of the tracked RNA and at the indicated time points. Bars, 10 μm.

(C) A model for the biogenesis and trafficking of MLV (see text). Violet star, budding machinery of internal vesicles of multivesicular bodies.

Immunoisolation of Vesicles

Cells were resuspended in TG buffer and broken with a ball-bearing cell-cracker (15 million cells per immunoisolation). Following centrifugation at 800 × g for 10 min, vesicles in the supernatant were purified by centrifugating at 100,000 × g for 1 hr on a cushion of TG buffer containing 20% sucrose. Vesicles were then resuspended in TG buffer containing 5% FBS and incubated at 4°C for 1–4 hr with either protein-G dynabeads (Dynal, Oslo, NO) coated with a goat anti-MA antibody, or with streptavidine dynabeads coated with biotylinated oligonucleotides (same as those used with in situ hybridization experiments, or with a control oligo that had a similar Tm). Unbound material was removed by three washes in TG buffer containing 1% BSA and two washes in TG buffer alone. Bound vesicles were then eluted in 1% SDS and adjusted in 1× Laemli buffer. TG is 10 mM HEPES-KOH, pH 7.2, 250 mM sucrose, 1 mM EDTA, and 1 mM $Mg(OAc)_2$.

Acknowledgments

We thank M. Zerial for the gift of Rab4- and Rab11-YFP and -CFP plasmids, B. Goud for Rab6-CFP, A. Benmerah for the dominant-negative Eps15 mutants, F.L. Cosset for HT-Fly and Fly E cells, and V. Kalatzis for the cystinosin-GFP vector. We are also grateful to M. Vidal, J.L. Battini, A. Blangy, and C. Gauthier for their extensive advice, and to N. Taylor for critical readings of the manuscript. This work was supported by grants from AFM, MNRT (ACI), Ensemble contre le SIDA, ANRS, ARC, and the EMBO YIP program. E. Basyuk was supported by a fellowship from Ensemble contre le SIDA.

Received: December 2, 2002
Revised: May 1, 2003
Accepted: May 8, 2003
Published: July 7, 2003

References

Benmerah, A., Bayrou, M., Cerf-Bensussan, N., and Dautry-Varsat, A. (1999). Inhibition of clathrin-coated pit assembly by an Eps15 mutant. J. Cell Sci. *112*, 1303–1311.

Bertrand, E., Chartrand, P., Schaefer, M., Shenoy, S.M., Singer, R.H., and Long, R.M. (1998). Localization of ASH1 mRNA particles in living yeast. Mol. Cell *2*, 437–445.

Carson, J., Worboys, K., Ainger, K., and Barbarese, E. (1997). Translocation of myelin basic protein mRNA in oligodendrocytes requires microtubules and kinesin. Cell Motil. Cytoskeleton *38*, 318–328.

Cosset, F.-L., Takeuchi, Y., Battini, J., Weiss, R., and Collins, M. (1995). High-titer packaging cells producing recombinant retroviruses resistant to human serum. J. Virol. *69*, 7430–7436.

Egan, M., Carruth, L., Rowell, J., Yu, X., and Siliciano, R. (1996). Human immunodeficiency virus type 1 envelope protein endocytosis mediated by a highly conserved intrinsic internalization signal in the cytoplasmic domain of gp41 is suppressed in the presence of the Pr55gag precursor protein. J. Virol. *70*, 6547–6556.

Eisel, U., Reynolds, K., Riddick, M., Zimmer, A., Niemann, H., and Zimmer, A. (1993). Tetanus toxin light chain expression in Sertoli cells of transgenic mice causes alterations of the actin cytoskeleton and disrupts spermatogenesis. EMBO J. *12*, 3365–3372.

Freed, E.O. (1998). HIV-1 Gag proteins: diverse functions in the virus life cycle. Virology *251*, 1–15.

Fusco, D., Accornero, N., Lavoie, B., Shenoy, S., Blanchard, J., Singer, R., and Bertrand, E. (2003). Single mRNA molecules demonstrate probabilistic movement on microtubules in living mammalian cells. Curr. Biol. *13*, 161–167.

Galli, T., Chilcote, T., Mundigl, O., Binz, T., Niemann, H., and De Camilli, P. (1994). Tetanus toxin-mediated cleavage of cellubrevin impairs exocytosis of transferrin receptor-containing vesicles in CHO cells. J. Cell Biol. *125*, 1015–1024.

Garoff, H., Hewson, R., and Opstelten, D. (1998). Virus maturation by budding. Microbiol. Mol. Biol. Rev. *62*, 1171–1190.

Garrus, J., von Schwedler, U., Pornillos, O., Morham, S., Zavitz, K., Wang, H., Wettstein, D., Stray, K., Cote, M., Rich, R., et al. (2001). Tsg101 and the vacuolar protein sorting pathway are essential for HIV-1 budding. Cell *107*, 55–65.

Gheysen, D., Jacobs, E., de Foresta, F., Thiriart, C., Francotte, M., Thines, D., and De Wilde, M. (1989). Assembly and release of HIV-1 precursor Pr55gag virus-like particles from recombinant baculovirus-infected insect cells. Cell *59*, 103–112.

Hansen, M., Jelinek, L., Whiting, S., and Barklis, E. (1990). Transport and assembly of gag proteins into Moloney murine leukemia virus. J. Virol. *64*, 5306–5316.

Jankovics, F., Sinka, R., and Erdelyi, M. (2001). An interaction type of genetic screen reveals a role of the Rab11 gene in oskar mRNA localization in the developing *Drosophila melanogaster* oocyte. Genetics *158*, 1177–1188.

Kloc, M., Zearfoss, N.R., and Etkin, L. (2002). Mechanisms of subcellular mRNA localization. Cell *108*, 533–544.

Lippincott-Schwartz, J., and Fambrough, D.M. (1987). Cycling of the integral membrane glycoprotein, LEP100, between plasma membrane and lysosomes: kinetic and morphological analysis. Cell *49*, 669–677.

Lodge, R., Delamarre, L., Lalonde, J.P., Alvarado, J., Sanders, D.A., Dokhelar, M.C., Cohen, E.A., and Lemay, G. (1997). Two distinct oncornaviruses harbor an intracytoplasmic tyrosine-based basolateral targeting signal in their viral envelope glycoprotein. J. Virol. *71*, 5696–5702.

McDonald, D., Vodicka, M.A., Lucero, G., Svitkina, T.M., Borisy, G.G., Emerman, M., and Hope, T.J. (2002). Visualization of the intracellular behavior of HIV in living cells. J. Cell Biol. *159*, 441–452.

Perotti, M., Tan, X., and Phillips, D. (1996). Directional budding of human immunodeficiency virus from monocytes. J. Virol. *70*, 5916–5921.

Ploubidou, A., and Way, M. (2001). Viral transport and the cytoskeleton. Curr. Opin. Cell Biol. *13*, 97–105.

Raposo, G., Moore, M., Innes, D., Leijendekker, R., Leigh-Brown, A., Benaroch, P., and Geuze, H. (2002). Human marophages accumulate HIV-1 particles in MHC II compartments. Traffic *3*, 718–729.

Reddy, A., Caler, E.V., and Andrews, N.W. (2001). Plasma membrane repair is mediated by Ca^{2+}-regulated exocytosis of lysosomes. Cell *106*, 157–169.

Saxton, W. (2001). Microtubules, motors, and mRNA localization mechanisms: watching fluorescent messages move. Cell *107*, 707–710.

Smith, G., and Enquist, L. (2002). Breaks in and breaks out: viral interactions with the cytoskeleton of mammalian cells. Annu. Rev. Cell Dev. Biol. *18*, 135–161.

Somsel Rodman, J., and Wandinger-Ness, A. (2000). Rab GTPases coordinate endocytosis. J. Cell Sci. *113*, 183–192.

Strack, B., Calistri, A., Accola, M., Palu, G., and Gottlinger, H.G. (2000). A role for ubiquitin ligase recruitment in retrovirus release. Proc. Natl. Acad. Sci. USA *97*, 13063–13068.

Suomalainen, M., Hultenby, K., and Garoff, H. (1996). Targeting of Moloney murine leukemia virus gag precursor to the site of virus budding. J. Cell Biol. *135*, 1840–1852.

Weclewicz, K., Ekstrom, M., Kristensson, K., and Garoff, H. (1998). Specific interactions between retrovirus Env and Gag proteins in rat neurons. J. Virol. *72*, 2832–2845.

Wilkie, G., and Davis, I. (2001). *Drosophila* wingless and pair-rule transcripts localize apically by dynein-mediated transport of RNA particles. Cell *105*, 209–219.